

PAPER • OPEN ACCESS

Interactions of CaO with pure Mg and Mg-Ca alloys—an *in situ* synchrotron radiation diffraction study

To cite this article: B Wiese *et al* 2024 *J. Phys. Mater.* **7** 035008

View the [article online](#) for updates and enhancements.

You may also like

- [Effect of Zn Existence on Mg Corrosion Due to Cu](#)
Hiroaki Ishimaru, Taiki Morishige and Toshihide Takenaka
- [Stable Structure and Electronic Structure for Mg\(Mg_xV_{1-x}\)₂O₄ As Cathode Material for Magnesium Secondary Battery in Discharge Process Using First-Principle Calculation](#)
Chiaki Ishibashi, Natsumi Kawakami, Naoya Ishida *et al.*
- [Characterization of Mg₂Zn_{1-x}O Films Grown by Remote-Plasma-Enhanced Metalorganic Chemical Vapor-Deposition using *bis*-Ethylcyclopentadienyl Magnesium](#)
Atsushi Nakamura, Kenji Yamamoto, Junji Ishihara *et al.*

PRIME
PACIFIC RIM MEETING
ON ELECTROCHEMICAL
AND SOLID STATE SCIENCE

HONOLULU, HI
October 6-11, 2024

Joint International Meeting of
The Electrochemical Society of Japan
(ECS)
The Korean Electrochemical Society
(KECS)
The Electrochemical Society (ECS)

Early Registration Deadline:
September 3, 2024

**MAKE YOUR PLANS
NOW!**



PAPER

OPEN ACCESS

RECEIVED

9 January 2024

ACCEPTED FOR PUBLICATION

17 April 2024

PUBLISHED

4 July 2024

Original content from this work may be used under the terms of the [Creative Commons Attribution 4.0 licence](#).

Any further distribution of this work must maintain attribution to the author(s) and the title of the work, journal citation and DOI.



Interactions of CaO with pure Mg and Mg-Ca alloys—an *in situ* synchrotron radiation diffraction study

B Wiese^{1,*} , C L Mendis² , D Tolnai¹ and N Hort^{1,3}

¹ Helmholtz-Zentrum Hereon, Institute of Metallic Biomaterials, Functional Magnesium Materials, Max-Planck-Straße 1, D-21502 Geesthacht, Germany

² Brunel Centre for Advanced Solidification Technology Brunel University London, Kingston Lane, Uxbridge UB8 3PH, United Kingdom

³ Leuphana University Lüneburg, Institute of Product Technology and Systems, Universitätsallee 1, D-21335 Lüneburg, Germany

* Author to whom any correspondence should be addressed.

E-mail: bjoern.wiese@hereon.de

Keywords: Mg-based alloys, *in situ*, synchrotron diffraction, Mg-Ca-O system, Eco-Mg

Abstract

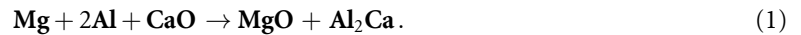
CaO additions are used as an inexpensive replacement for Ca in Mg alloys. CaO dissociation in Mg has been reported in literature without a clear mechanism as to why this occurs. *In situ* synchrotron radiation diffraction investigation of the melting and solidification of Mg with CaO shows, that the stability of CaO was overestimated in Mg melts compared with MgO. The experiments that were performed on the Mg-20CaO and Mg-*x*Ca-6CaO (*x* = 6 and 16 wt.%) alloys, show the dissociation and formation of various phases during melting and solidification. The results indicate that Mg can reduce CaO even in the solid state, which is the opposite of that proposed by the Ellingham diagrams for stoichiometric reaction. Phase formations during the *in situ* experiment are compared with published thermodynamic calculations for the interaction between Mg-Ca alloys and oxides.

1. Introduction

Investigations on the oxidation behaviour of Mg-Ca alloys show an increase in the high temperature resistance. This increase persists until an elevated temperature of 645 °C at a Ca concentration of 0.2 wt.% [1]. However, the effect of Ca in increasing this oxidation resistance is not well understood. The Standard Gibbs free energy change (ΔG°) associated with CaO [2] is lower than that for MgO per mole of O₂ at any given temperature. Thus, CaO should remain more stable and the MgO formation at the expense of CaO is not thermodynamically possible. Gourishankar *et al* [3] reported that CaO is less stable than MgO, which affects the hypothesis provided for the protective nature of CaO. The increment of the oxidation protection at high temperatures is due to the increased density of the oxide layer, but the exact nature of this is not fully understood. The Pilling Bedworth Ratio (PBR) [4] of Ca/CaO is lower than of Mg/MgO so that this cannot be used by itself to explain this improvement by forming a compact oxide layer. High temperature applications require sufficient oxidation resistance and mechanical properties to extend the range of application. These Mg-Ca alloys improved the safety during production as well as during further processing at elevated temperatures. Another approach is to use of CaO as a cost-efficient alloying addition for Mg alloys, as a replacement for Ca. The investigations in to the development of *ECO-Mg* (*Environment CONscious magnesium*) [5–7] do not provide an explanation for the dissociation of CaO in Mg alloys or the exact nature by which CaO additions increase the oxidation resistance. A detail review of *ECO-Mg* can be found in Rafiei *et al* [8].

Previous investigations show that the dissociation of CaO occurs in Mg alloys, which indicate that CaO is less stable than MgO or that some more stable phases form. Kondoh *et al* [9] proposed a calculation to explain the dissociation of CaO in Mg-Al alloys, and used the ΔG° for the reaction between Mg-Al alloys and CaO. They calculated a negative ΔG° for the reaction in equation (1) indicating the products to be more stable compared to the reactants. They suggest that during the reaction between pure Mg and CaO ΔG° is close to zero at approximately 150 °C, and more positive with increasing temperature. Thus, Mg + CaO

should be stable, but this do not consider the enthalpy of mixtures. However, this explanation is based on the experimental results of AZ61 mechanically alloyed with CaO and subsequently heat treated to consolidate the mixture. This investigation showed the formation of Al_2Ca and not the dissociation of CaO, with any possible intermediate steps



An investigation on the phase transformation between an Mg alloy and CaO, the standard techniques, e.g. differential scanning calorimetry (DSC) or differential thermal analysis (DTA), are not adequate tools to follow the phase transformation over the temperature range. These techniques use the change in energy for the detection of the phase transformation but provide no information on the phases involved in a reaction. If a number of phases transform at similar temperatures, it is not possible to distinguish between them.

One way to understand the interactions between Mg and CaO is to understand the thermodynamic basis behind such reactions. Schmid-Fetzer *et al* [10], Liang *et al* [11] and Jung *et al* [12] calculated the thermodynamic equilibria in ternary Mg-Ca-O system using the thermodynamic software Pandat and FactStage with a combined thermodynamic database for metals and oxides, respectively. Jung *et al* [12] predicted that CaO is not stable in molten Mg, up to 13 wt.% CaO and is reduced by Mg to MgO. At a higher amount of CaO (>13 wt.% in molten Mg) both MgO and CaO will be stable in the melt. This thermodynamic calculations [10] provided for the first time a thermodynamically based explanation as to why CaO is not stable in molten Mg.

High-energy x-ray diffraction has been utilised in this investigation to observe various interactions between Mg and CaO *in situ* in number of different materials, e.g. phase evolution of Mg alloys during solidification [13, 14], elevated temperature compression [15, 16] and dissolution of CaO during heating [17, 18]. *In situ* experimental set-up allows detect phase identification of phases during a phase transformation with a useful time temperature resolution. This type of investigations provides the transformations involved with the dissociation of CaO. This paper contributes to the understanding on the phase transformation associated with the reduction of CaO during heating and solidification in combination with Mg. As part of the investigation, the validity of the stability the CaO and MgO in the ternary Mg-Ca-O system is also examined. For this purpose, *in situ* synchrotron radiation diffraction experiments were conducted during melting and solidification. The *in situ* and *ex situ* experiments were performed on the Mg-CaO and Mg-Ca-CaO alloys. The phase formations during the experiment are compared with thermodynamic modelling of phase evolutions. The thermodynamic calculations used from the work from Liang *et al* [11] and Jung *et al* [12]. Results from this work were the initiator for the study of Schmid-Fetzer *et al* [10] and were used to validate the thermodynamic calculations of Schmid-Fetzer *et al* [10] and Liang *et al* [11].

2. Experimental procedure

2.1. Sample preparation

An Mg-20CaO sample containing pure Mg (99.99%) with 20 wt.% CaO powder (Calcium oxide 96% powder from CARL ROTH, Germany), and the Mg- x Ca + 6CaO samples contain the master alloys Mg-6Ca and Mg-16Ca with 6 wt.% CaO powder were used for the interaction study with CaO. In addition, pure Mg were prepared and analysed using the same method in order to evaluate the temperature accuracy of the set-up. The pure Mg and the Mg-Ca master alloy chips were produced by cutting cast alloy samples. The CaO was dried for 6 h at 350 °C remove any moisture attached to the CaO. The chips were mixed with the CaO powder for 3 min in a glass container (15 ml) by hand to create a uniform mixture of the white CaO and metallic Mg. This transparent container allows visual control of the mixture during the mixing process. Then the mixture was pressed with a hydraulic press into cylinders with a diameter of 4 mm and a height of approximately 4 mm, under an applied pressure of 100 MPa for 1 min. Mixing and pressing were performed in glove boxes in a controlled atmosphere with a concentration of H_2O and O_2 lower than 0.1 ppm. The samples were stored in containers in an argon atmosphere until the measurements were performed.

2.2. Composition of the Mg chips

For composition measurements, Mg and Mg-Ca alloy chips were pressed with a hydraulic press to cylinders with a diameter of 4.0 mm, under an applied pressure of 500 MPa and held for 1 min. The compositions were measured by analysing the three samples at three different places using scanning electron microscopy (SEM) (TESCAN VEGA III, operating at 20 kV) associated with energy-dispersive x-ray spectrometry (EDXS).

2.3. *In situ* synchrotron radiation diffraction measurement

The *in situ* studies were conducted at the High Energy Materials Science beamline P07 (HEMS) at PETRA III of DESY (Deutsches Elektronen-Synchrotron), Hamburg, Germany [19]. The synchrotron radiation

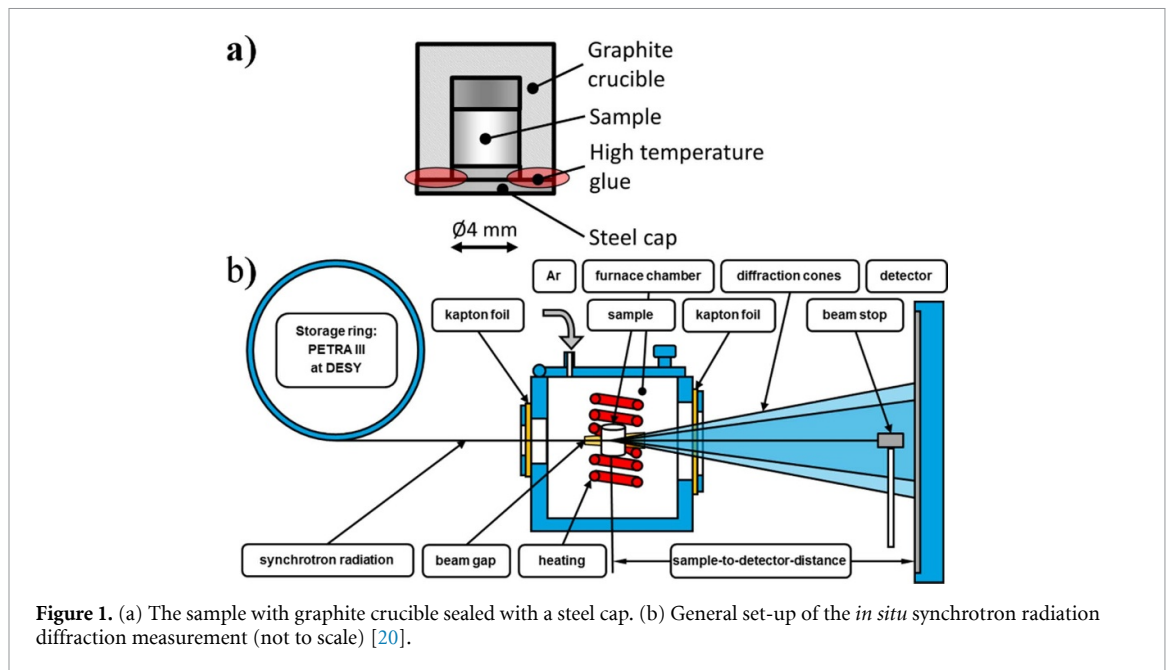


Figure 1. (a) The sample with graphite crucible sealed with a steel cap. (b) General set-up of the *in situ* synchrotron radiation diffraction measurement (not to scale) [20].

diffraction study was conducted with a beam energy of 100 keV (wavelength of $\lambda = 0.0124$ nm). The beam cross section was set to 1.0×1.0 mm². The synchrotron radiation experimental set-up is shown in figure 1.

The experiment was conducted in a furnace with a modified induction coil so that the x-ray beam passes without hindrance. The samples, contained in a graphite crucible (diameters 4 mm, height 4 mm) with a steel cap, were heated in an Ar atmosphere to 750 °C at 10 K min⁻¹, held at this temperature for 5 min to ensure melt homogeneity, and then cooled at 10 K min⁻¹ to 200 °C (fully solidified state) before air-cooling to room temperature (min. 590 patterns over ~120 min). The cap is on the bottom to ensure that the samples were in contact with the lid (figure 1(a)). This allowed the heat to flow to the thermocouple, which has to be welded to the steel cap for temperature control. The samples were prepared in ambient conditions and the steel lid was held in place with high temperature silicone glue (Thermocoll (1100 °C)). The crucible with the sample was rotated by 90° during a 1 s acquisition to improve statistics.

The two dimensional (2D) diffraction patterns were recorded in transmission geometry with a PerkinElmer XRD 1622 flat panel (pixel size of 200 μ m²) at a sample-to-detector-distance of 1162.7 mm (calibrated with a LaB₆ reference), as illustrated in figure 1(b). The patterns were recorded every 12 s with an acquisition time of 1 s, allowing a temperature resolution of 2 °C. X-ray line profiles were obtained by azimuthal integration of the 2D diffraction patterns through 360° using FIT2D V12.077™ software. For phase identification simulated line profiles were generated with CaRIne 3.1 Crystallography™ with crystal structure data from the Pearson's Crystallography Database [21].

2.4. Metallographic investigation

Samples for scanning electron microscopy were embedded in epoxy resin and ground with 350–2500 grit SiC paper then polished first with 3 μ m diamond suspension and finally with a mixture of 1 μ m diamond and SiO₂ OPS (Oxide Polishing Suspension) (Cloeren Technology GmbH, Wegberg, Germany) anhydrous suspension. Microstructures were investigated with a scanning electron microscope (SEM, TESCAN VEGA III, Brno, Czech Republic) equipped with an energy-dispersive x-ray spectroscopy (EDXS, IXRF Systems, IXRF, Austin, USA) with the Iridium Ultra software (IXRF, Austin, USA). The compositions of the investigated regions are shown as compositional maps with the quantitative composition calculated as wt.%.

3. Results

3.1. Composition of the chips

The Mg, Ca and O content of the pure Mg and the pure Mg-Ca master alloys chips was measured with SEM-EDXS, table 1. The three alloys having an increased oxygen content most likely due to the surfaces oxidation during sample preparation. The measurements show that there is some MgO found.

Table 1. The measured composition for pure Mg, Mg-6Ca and Mg-16Ca chips with the average over three measurements and standard deviation of the EDXS measurement.

Sample	Composition	Ca (wt.%)	O (wt.%)	Mg (wt.%)
Pure Mg	Average	—	2.3	97.7
	Standard deviation	—	0.2	0.2
Mg-6Ca	Average	4.9	3.93	91.1
	Standard deviation	0.2	0.2	0.3
Mg-16Ca	Average	15.1	6.0	78.9
	Standard deviation	0.6	0.3	0.8

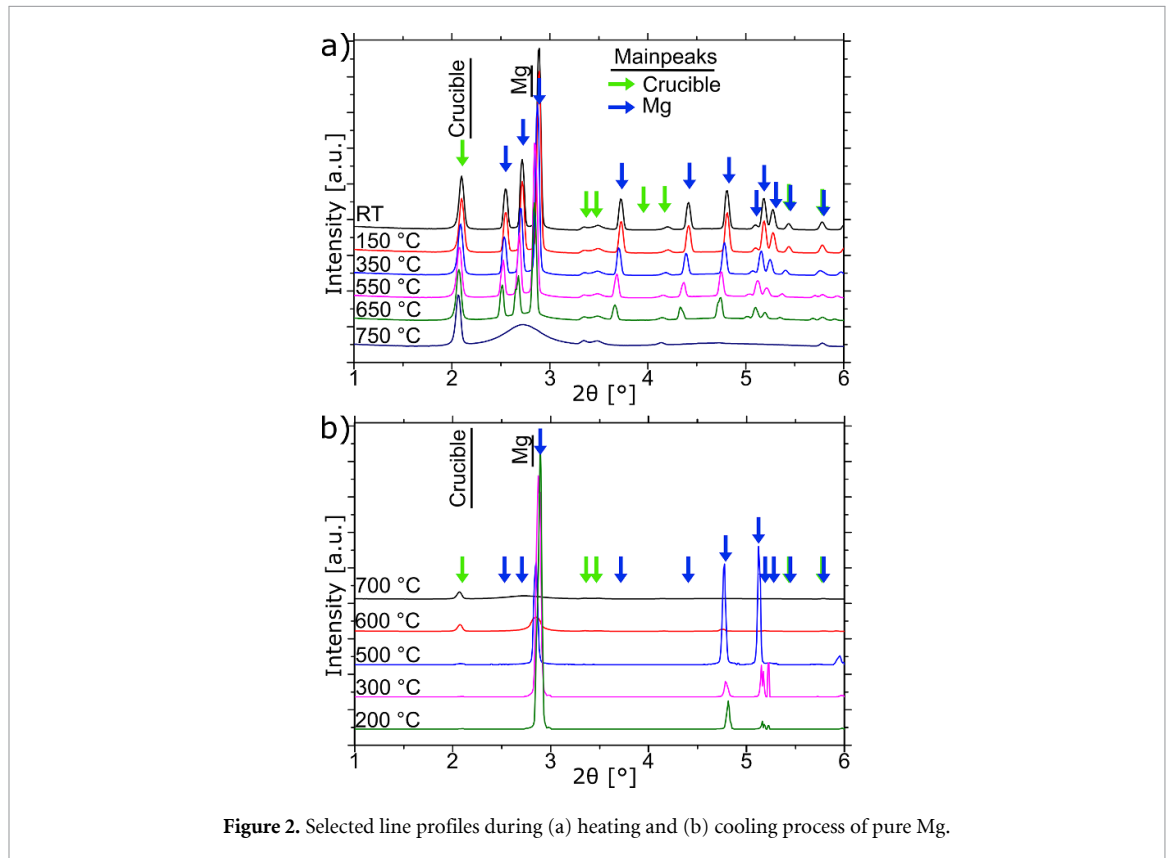


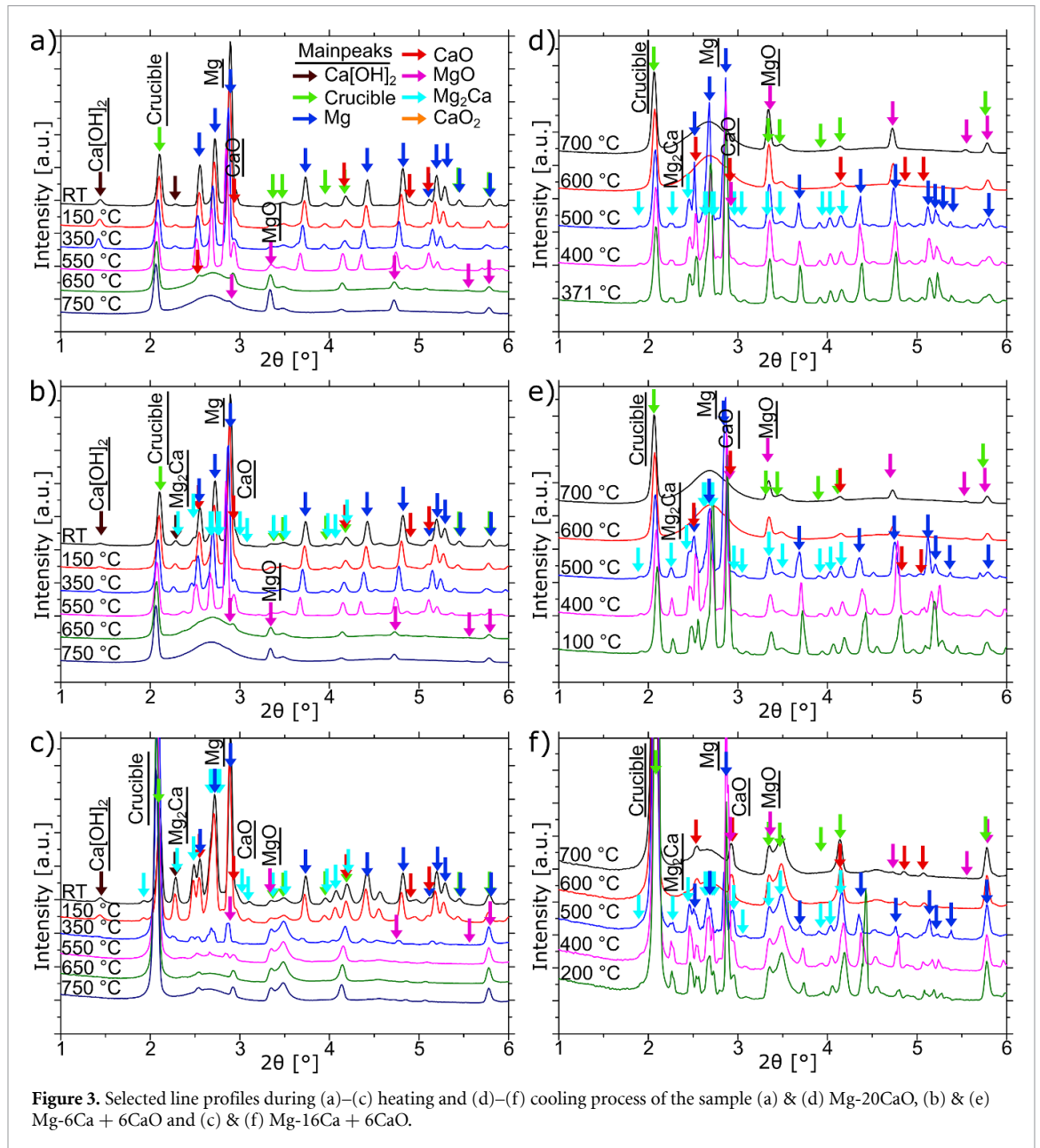
Figure 2. Selected line profiles during (a) heating and (b) cooling process of pure Mg.

3.2. *In situ* results

The synchrotron results on the pure Mg sample (table 2 and figure 2) show a melting temperature above 650 °C. From 652 °C, the intensity of the Mg peaks decreases rapidly, and at 654 °C no more intensity could be determined. Above this temperature, the samples show the diffraction peaks of the graphite crucible and a diffuse background, which can be attributed to molten Mg. No change can be detected during the holding time. The first Mg peaks appear during solidification at 649 °C, and solidification ends at 647 °C.

The x-ray line profiles in figure 3 and the analysed results in table 2 show that peaks due to $\text{Ca}[\text{OH}]_2$, CaO, Mg and graphite crucible and for Mg-Ca alloys also Mg_2Ca are found at the beginning of the experiment. During heating of Mg-20CaO the main peak of CaO becomes more visible above 291 °C, due to the thermal expansion of Mg. This trend was not as pronounced in the Mg-Ca alloys, but the intensity of the CaO peak increased in all three samples up to a maximum temperature at about 500 °C. Only in the case of Mg-20CaO stabilisation of the intensity of the CaO peaks was observed between 291 °C and 396 °C. The peaks of $\text{Ca}[\text{OH}]_2$ start to disappear at 408 °C and are undetectable at 500 °C for Mg-20CaO. With more Ca in metallic form, disappearance of $\text{Ca}[\text{OH}]_2$ starts at lower temperatures between 234 °C and 382 °C for Mg-16Ca + 6CaO.

During heating the peaks of MgO are detected at a temperature of 340 °C, 486 °C and 481 °C for Mg-20CaO, Mg-6Ca + 6CaO and Mg-16Ca + 6CaO respectively. The tendency for the appearance of MgO is opposite to that of the disappearance of $\text{Ca}[\text{OH}]_2$ and increases with the Ca content in metallic form. However, this stabilises with increased metallic Ca at higher temperatures. The peaks of CaO starts to



decrease in Mg-16Ca + 6CaO at the same temperature as the MgO peaks were first detected, at 481 °C. The peak intensity of CaO begins to decrease at 568 °C and 589 °C for Mg-20CaO and Mg-6Ca + 6CaO alloys respectively. Therefore, the disassociation of CaO in both samples were detected at higher temperatures than the first formation of MgO. The stabilisation of the CaO and MgO peaks are at similar temperatures and increasing with more metallic Ca.

In the temperature range between 620 °C and 637 °C the Mg peaks disappear for Mg-20CaO and for the alloys with higher Ca content at lower temperatures, between 500 °C and 600 °C. With the disappearance of Mg peaks, the diffuse scattering of the melt was detected. The peaks of the Laves phase Mg₂Ca decrease from a temperature of 497 °C to 512 °C to zero for both Mg-Ca alloys.

During cooling the first peaks of Mg are detected at 570 °C in Mg-20CaO and for the Mg-6Ca + 6CaO and Mg-16Ca + 6CaO at 581 °C and 533 °C, respectively. No intensity changes in Mg or oxides peaks were detected between 509 °C and 504 °C for all samples. The Laves phase Mg₂Ca was detected between 511 °C and 504 °C.

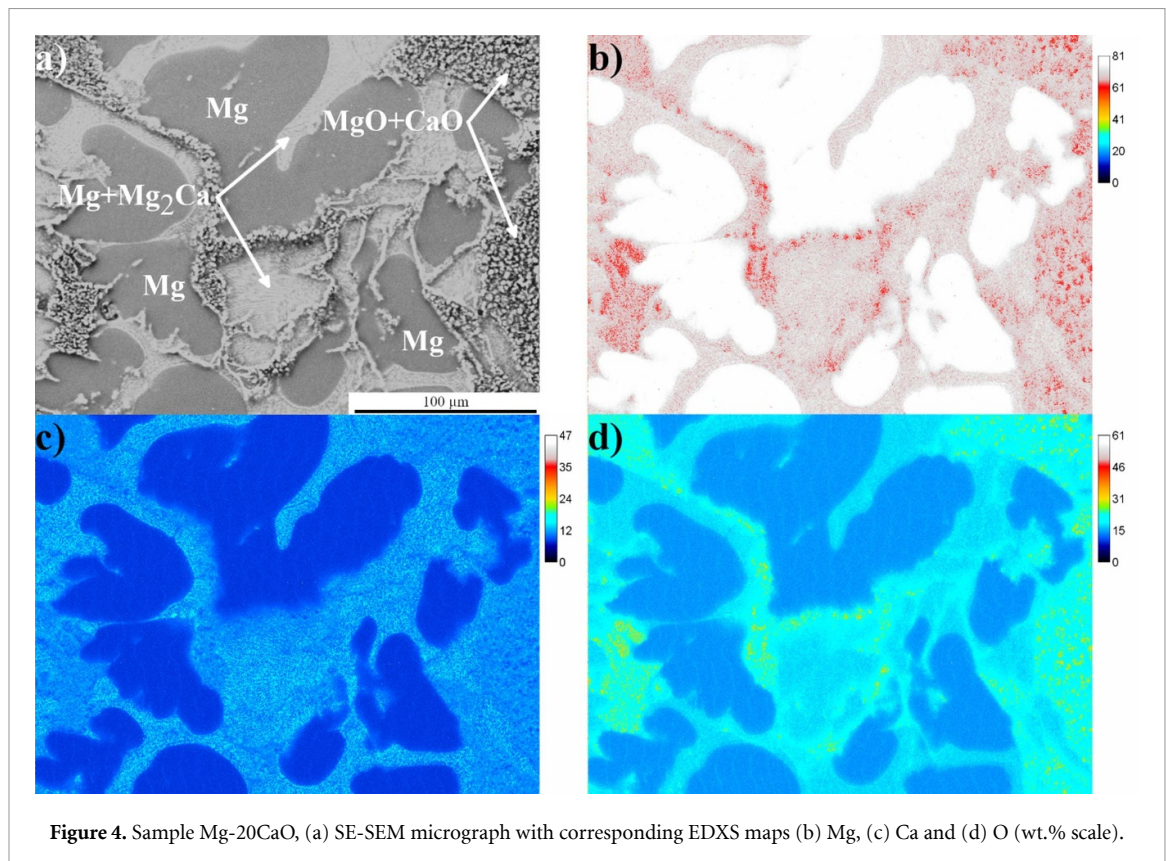
3.3. Microstructures

The microstructures of the alloy samples subjected to solidification studies were analysed with SEM. The EDXS maps show the distribution of Mg, Ca and O in the solidified samples. As an example, in the Mg-20CaO sample shown in figures 4 and 5 shows the secondary electron micrographs of Mg-6Ca + 6CaO

Table 2. Temperatures at which disappearance and appearance of various phases are detected during heating and cooling for pure Mg and alloys with nominal compositions of Mg-20CaO, Mg-6Ca + 6CaO and Mg-6Ca + 16CaO. The temperatures are accurate to ± 5 , which is a result of the experimental set-up and setting.

	Reaction samples	Pure Mg	Mg-20CaO	Mg-6Ca + 6CaO	Mg-16Ca + 6CaO
Heating	Disappearance Ca[OH] ₂ start	—	408	350	234
	Disappearance of Ca[OH] ₂ end	—	500	433	382
	Increment of CaO start	—	20	20	20
	Increment of CaO end (stable)	—	291	—	—
	Increment of CaO start 2	—	396	—	—
	Increment of CaO end (max.)	—	502	589	481
	Decrement CaO start &	—	568	589	481
	Decrement of CaO end (stable)	—	664	671	750
	Appearance of MgO start	—	340	486	481
	Appearance of MgO end (stable)	—	618	675	759
	Disappearance of Mg start	652	620	504	497
	Disappearance of Mg end	655	637	602	574
	Disappearance of Mg ₂ Ca start	—	—	504	497
	Disappearance of Mg ₂ Ca end	—	—	506	512
Cooling	Appearance of Mg start	649	570	581	533
	Appearance of Mg end	647	509	504	507
	Appearance of Mg ₂ Ca start	—	511	504	510
	Appearance of Mg ₂ Ca end	—	509	504	507

Temperature (°C)



and Mg-16Ca + 6CaO with regions containing various phases, respectively. The regions are labelled according to the results from the EDXS maps. All the samples have a similar microstructure with Mg as primary phase that during the later stages of solidification solidifies with a lamellar eutectic structure of Mg and Mg₂Ca during the eutectic solidification. The O agglomerates in the eutectic regions as clusters of oxide particles, this agglomeration show slight differences in the distribution of Ca. According to the microstructures with the differences in the distribution of Ca the samples can be separated in to two groups.

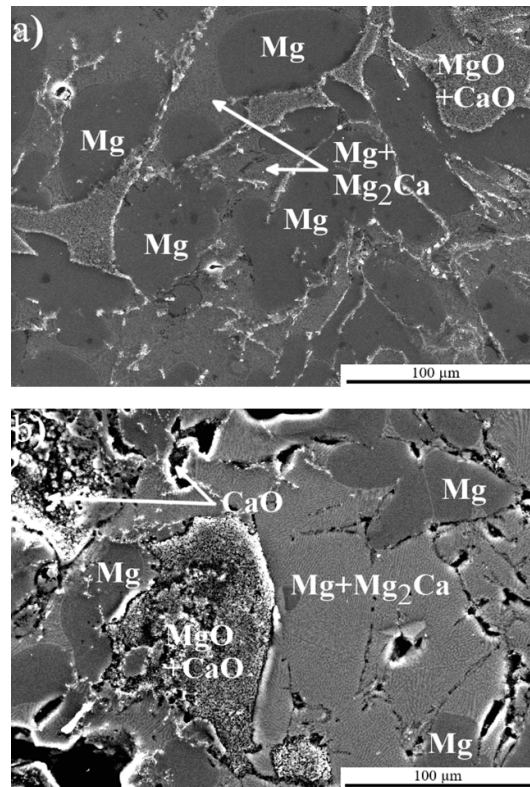


Figure 5. SE-SEM micrograph of (a) Mg-6Ca + 6CaO and (b) Mg-16Ca + 6CaO with corresponding regions of Mg, eutectic Mg + Mg₂Ca, MgO and CaO regions (determined by EDXS maps).

Table 3. Nominal and EDXS with standard deviation measured ternary Mg-Ca-O sample compositions investigated in this study.

Sample	Composition	Mg (wt.%)	Ca (wt.%)	O (wt.%)
Mg-20CaO	Nominal	80.0	14.3	5.7
	EDXS	84.5	6.8 ± 1.4	8.7 ± 1.7
Mg-6Ca + 6CaO	Nominal	88.4	9.9	1.7
	EDXS	87.0	8.2 ± 1.6	4.8 ± 1.0
Mg-16Ca + 6CaO	Nominal	79.0	19.3	1.7
	EDXS	78.6	15.3 ± 3.1	6.1 ± 1.2

The sample Mg-16Ca + 6CaO with a large region of CaO separated from the MgO + CaO regions. Mg-20CaO and Mg-6Ca + 6CaO shows only with regions of MgO + CaO.

The composition of the three samples were analysed with SEM-EDXS, due to small sample size, to determine the relationship between the actual and nominal compositions. The SEM-EDXS composition measured deviates from the nominal compositions, which are listed in table 3.

4. Discussion

Mg melts between 652 °C and 654 °C and solidifies between 650 °C and 647 °C. According to the literature, the melting temperature of Mg is 650 °C [22] and from this we derive a measurement accuracy of ±5 °C in this experimental setup. The delay in the melting and solidification process is due to the kinetics associated with the nucleation growth or disassociation of Mg crystals. This is related to the time and energy required for the Mg atoms to reorganise for the phase transition from solid to melt and vice versa. As a result, the temperature appears to be higher than the literature values for heating and lower than the values for cooling. It is also possible that the heat flow from the sample through the lid to the thermocouple causes a slight deviation in temperature due to heat transport and the higher heat capacity of the steel lid compared to the Mg sample. The O content of the pure Mg chips has no influence on the solidification temperature during heating and cooling. The non-statistical distributions of the peaks show in figure 2 that only a few Mg crystals are in the Bragg state. This is due to the small number of nucleation sites in pure Mg, which

minimise the number of grains in the measured volume. This is also related to the slower cooling rate and grain growth, which lead to a non-random distribution of grain orientations.

The evaluation of volume fractions using Rietveld refinement was not possible with the available results. This was since the reflections of the graphite crucibles interfered with the evaluation to such an extent that we were unable to reliably correlate the signal change with the volume change. In order to be able to compare such measurements more comprehensively with volume fractions from e.g. thermodynamic simulations or tomography data, these should be taken into account in future studies.

The x-ray line profiles confirm the presence of $\text{Ca}[\text{OH}]_2$ and CaO for all samples. The $\text{Ca}[\text{OH}]_2$ forms during sample preparation due to the highly hydrophilic nature of CaO [23]. The $\text{Ca}[\text{OH}]_2$ dissociates before Mg and Mg-Ca alloys are melted. The dissociation temperature for $\text{Ca}[\text{OH}]_2$ is at 512°C [23]. In Mg-20CaO, the dissociation of $\text{Ca}[\text{OH}]_2$ started at 408°C , and this phase disappeared completely by 500°C . In Mg-6Ca + 6CaO the dissociation of $\text{Ca}[\text{OH}]_2$ was observed between 350°C and 433°C , and in Mg-16Ca + 6CaO between 234°C and 382°C . The literature values for dissociation of $\text{Ca}[\text{OH}]_2$ are for the pure compound and not in presence of Mg or Mg alloys. It is possible that the presence of Mg decrease the temperature for the dissociation of $\text{Ca}[\text{OH}]_2$, due to a catalytic influence of metallic components. The same amount of CaO and $\text{Ca}[\text{OH}]_2$ was dissociated faster in the Mg-16Ca + 6CaO sample than in the Mg-6Ca + 6CaO sample may be due to the increased amount of Ca in the alloy.

When $\text{Ca}[\text{OH}]_2$ starts to dissociate, the first peaks of MgO were also detected in Mg-20CaO. The peaks of MgO were detected in Mg-6Ca + 6CaO at 486°C and Mg-16Ca + 6CaO at 481°C both higher temperatures, than in Mg-20CaO at 340°C . This is related to a lower driving force for the reduction of CaO due to the lower amount of O in the Mg-xCa + CaO samples. So that Mg reacts with the O out of $\text{Ca}[\text{OH}]_2$. In the last steps, CaO dissociates and reacts to MgO, but with a leftover of CaO if the CaO content is higher.

According to the literature the melting temperature of pure Mg is 650°C [22]; the experiment shows melting to start at 620°C for Mg-20CaO. The lower value of incipient melting indicates that solid-state reaction between Mg and Ca containing phases must have occurred at an earlier temperature. The thermodynamic calculation of Liang *et al* [11] also confirm this findings, where MgO is more stable than CaO at low temperate and at elevated temperatures MgO and CaO are stable in the presence of Mg. Depending on the concentration Ca and O Liang *et al* predict the formation of just MgO at low or MgO and CaO at higher concentrations of Ca and O. After Mg starts reducing CaO , Ca diffuses into solid Mg. This leads to the observation of reduced solidus temperature due to the solubility of Ca in Mg as shown in Mg-Ca system, without the formation of Mg_2Ca is in perfect agreement with the present observations.

The experimental data for Mg-20CaO in table 2 show the disappearance of Mg starts at 620°C and end at 637°C . The lower temperature is clearly related to the first formation of liquid, as discussed above for incipient melting. The higher temperature, 637°C , is because the presence of liquid phase will boost the kinetics of the Mg + CaO reaction. That results in more of the Ca becoming available, dissolving in the growing liquid phase in Mg-Ca alloy. The calculated liquids temperature of 637°C is obtained for 2.3 wt.% Ca in the liquid phase, corresponding to complete disappearance of Mg peaks observed during heating. This also explains why it is not necessary to assume the formation of Mg_2Ca during the Mg + CaO reaction as 2.3 wt.% Ca is below the eutectic liquid composition of 16.3 wt.% Ca.

It is noted that in an earlier work by Wiese *et al* [17] the Mg_2Ca Laves phase was not detected at 407°C during melting. This relates to the preparation of the sample in the previous investigations where Mg chips and CaO powder mixture were not compacted. The diffusion in the non-compacted Mg chips and CaO powder sample observed by Wiese *et al* [17] is close to unidirectional diffusion, due to the plate like geometry (2D) of the Mg chips. This causes the Ca concentration to reach a relatively high value close to the Mg/ CaO interface leading to the formation of Mg_2Ca phase. In this investigation compacted samples are likely to provide a multi-directional diffusion, thus only a solid solution forms. Thus, during the reaction between $\text{Mg}(\text{solid}) + \text{CaO}$ Ca diffuse into the solid Mg. When the Ca concentration is low a solid solution forms, when Ca concentration is above the solubility limit Mg_2Ca Laves phase form. In comparison to Wiese *et al* [17] it was possible to analyse the microstructure of the samples after the *in situ* experiment, which was advantageous for the validation and interpretation of the diffraction measurement.

The present investigation shows that pure Mg can reduce CaO even without the formation of the Laves phase, Mg_2Ca and molten Mg. This is in disagreement with the conclusion from Kondoh *et al* [9] that CaO is stable in the presence of pure Mg. Their thermodynamic calculations have number of short comings the first is that the thermodynamic calculations is the use of traditional thermodynamic data for the pure oxides, close to the Ellingham diagram data [24]. The second and the more fundamental problem is the use of chemical reaction equations among stoichiometric phases [9]. This approach is not capable to capture the actual dissolution process involving solid or liquid phases as opposed to the present treatment. The suggestion of Kondoh *et al* [9] for the dissociation of CaO in Mg-Al alloys cannot be applied here. In the present study, no Al-containing alloys were investigated, so that the formation of the very stable Laves phase

Al_2Ca cannot be considered as a thermodynamic driving force. It was found that this phase as well as the Mg_2Ca phase were not necessary to dissolve CaO. It is possibly due to the higher Standard Gibbs free energy of the stoichiometric reaction to Al_2Ca that Al cannot be dissolved in the Mg crystal and this Laves phase was formed in Kondoh *et al* [9].

$\text{Mg-6Ca} + 6\text{CaO}$ and $\text{Mg-16Ca} + 6\text{CaO}$ show a decrease in the intensity of the Mg_2Ca peak during heating. These two samples contain Mg_2Ca phase that formed during the solidification of these billets, as illustrated in figures 3(b) and (c) with the diffraction patterns between 350 °C and 550 °C. The explanation for this disappearance of the Mg_2Ca phase during heating due the increase of the solubility of Ca in Mg, thus the amount of Mg_2Ca must decrease. The eutectic reaction in the Mg-Ca system is at 516 °C [22] and is slightly above the range of accuracy determined with pure Mg. Three points may be responsible for the greater deviation in $\text{Mg-6Ca} + 6\text{CaO}$: 1. An too small volume of Mg_2Ca , 2. The kinetics during the conversion or 3. The heat transport. Since the values during heating and cooling are always below 516 °C, it can be assumed that this is case 1 and the amount of Mg_2Ca is low high. This conclusion is also consistent with the results for the pure Mg sample. However, it shows that the volume fraction can easily fall below the detection limit for two phases in this experimental setup.

The reduction or dissociation of CaO begins and ends for all with the content of CaO in the presence of MgO. This is in good agreement with the microstructural investigation, which still shows areas with MgO and CaO, and the diffractograms, with the diffraction signals of CaO. The reduction speed of CaO is higher and related to the higher diffusion rate in the molten state. The driving force for the reduction of CaO is lower due to the higher amount of Ca. The lower melting range leads to a faster increase of the liquid fraction in the sample, thus boosting the reaction kinetics. The phase formation temperatures for MgO (stabilisation of the intensity) and CaO (stabilisation of the intensity) occurs in both samples at the same temperature, so that the phase formation sequence is the same but it ends at a higher temperature with a higher Ca content. As proposed previously, the reaction products from around the CaO particles decrease the diffusion of Mg from the melt to these particles, which results in formation of CaO particles in the melt.

During solidification, an intensity change was not observed for MgO and CaO. The main oxide phase observed is MgO, as indicated by the higher intensity of the MgO peaks compared with that of the residual CaO. This indicates that MgO is more thermally stable compared with CaO in the investigated compositions of this ternary system. The small residual amount of CaO may be due to the reduction or disassociation reactions could not be completed during the heating cycle or only a fraction of CaO is disassociated in molten Mg. The thermodynamic calculations of Jung *et al* [12] also show that the disassociation of CaO in molten Mg at 700 °C will take place up to 13 wt.% of CaO in molten Mg, what is in an agreement with a leftover of CaO after the *in situ* experiment. According to the thermodynamic assessment of the ternary system Mg-Ca-O of the Liang *et al* [11] shows an transition from $\text{MgO} + \text{Liquid}$ over $\text{MgO} + \text{CaO} + \text{Liquid}$ to just $\text{CaO} + \text{Liquid}$ as stable oxide in this system with higher Ca and O content. Therefore, the residual of CaO can be attributed the stable phases $\text{MgO} + \text{CaO} + \text{Liquid}$ at in the molten state of the metallic components by thermodynamic reasons or to a slower reaction with a building MgO layer around the CaO by kinetic reasons.

Table 2 lists the solidification sequence of the Mg-20CaO , $\text{Mg-6Ca} + 6\text{CaO}$ and $\text{Mg-16Ca} + 6\text{CaO}$ samples with the start and end temperatures for various phase formations and stable oxides. The solidification begins with Mg and ends with the eutectic solidification of Mg and Mg_2Ca as detected with *in situ* synchrotron radiation measurements. The final solidification is the eutectic reaction related to the disappearance of the background from the molten metal and the appearance of Mg_2Ca . The *in situ* results from the three samples are in agreement with the SEM investigations (figures 4 and 5). The microstructure shows primary formation of Mg and the eutectic lamellar structure of Mg and Mg_2Ca . This microstructure is characteristic of the Mg rich side of the binary Mg-Ca system [25–27].

A shift in the ratio of these oxides was predicted by Liang *et al* [11] by thermodynamic calculations. This possible transformation of MgO into CaO or vice versa cannot take place due to the lack of solubility of O and therefore no diffusion in Mg, so that the intensity of the standing oxides does not change. This effect would not have been seen in standard thermo-analytical technique such as those made with differential scanning calorimetry (DSC) or differential thermal analysis (DTA) and shows the advantages of *in situ* measurement by diffraction.

The solidification ends with the formation of Mg_2Ca between 504 °C and 511 °C. The eutectic equilibrium temperature on the Mg rich side of the Mg-Ca system is calculated to be 516.5 °C based on critical review and thermodynamic assessment [28] of all available experimental data, including [25, 29–31]. The formation of Mg_2Ca occurs within the range of temperature error of ± 5 °C. However, the temperature at which Mg_2Ca forms is also likely to be associated with non-equilibrium cooling. The eutectic transformation of Mg and Mg_2Ca should not show a solidification range according to the phase diagram, but due to energy barriers associated with nucleation and growth of Mg and Mg_2Ca phases this is observed. As a

result, the solidification needs time, which leads to a lower temperature for the complete solidification. According to the results from Mg-6Ca + 6CaO, Mg-16Ca + 6CaO and from Mg-20CaO, the eutectic temperature is constant and oxygen only has a negligible effect on the formation temperature.

In each sample oxygen agglomerates in the eutectic region in a form of clusters of oxide particles. The SEM and EDXS results show a higher concentration of Mg in the O rich region of Mg-20CaO and Mg-6Ca + 6CaO compared with the O free region in the eutectic structures. In the as solidified microstructures, the O rich regions have a concentration of more than 50 wt.% Mg and less than 12 wt.% Ca, so that the main oxide is MgO for Mg-20CaO and Mg-6Ca + 6CaO. In the case of Mg-16Ca + 6CaO there are extra regions with mainly CaO (up to 75 wt.% Ca), which is in agreement with the calculation of Jung *et al* [12] or Liang *et al* [11] for molten Mg with a higher amount of CaO. Together with the synchrotron x-ray radiation diffraction results, these oxide rich regions are identified as MgO and a remainder CaO for the Mg-20CaO and Mg-6Ca + 6CaO and for the Mg-16Ca + 6CaO with extra regions with significant CaO. The Mg-16Ca + 6CaO sample has a higher Ca concentration than the other alloys in the O rich regions, but the main oxide phase remains MgO with a significant amount of CaO. The decrease in the intensity of CaO peaks is not as strong as with the other samples. The Mg nuclei grow and the MgO particles agglomerate in the liquid side of the solidification front. This moves the MgO particles out of the Mg grains, and clusters of these particles form in the melt. Below the eutectic temperature, the rest of the melt solidifies and encompasses the oxide particles between the eutectic structures. The type of four-phase reactions, $\text{Mg} + \text{Mg}_2\text{Ca} + \text{MgO} + \text{CaO}$, in the development of the non-equilibrium constitution could be explained by considering this *in situ* measurements in Liang *et al* [11] thermodynamic productions.

The microstructure, the location of the oxides in the eutectic structure and the *in situ* results indicate that MgO did not affect the solidification in the Mg-Ca system. Just the amount of Mg bonded as MgO will increase the amount of Ca in the liquid.

5. Conclusions

Compared to previous work, this work shows that *in situ* diffraction techniques are able to provide new insights into real dissolution and melting processes. They enable the identification of reactions that are not detectable with standard techniques or can provide new insights to validate thermodynamic databases and predictions. The main results of the experimental work show the role of CaO in the ECO-Mg and also in the Mg-Ca-O ternary system. The reductions of CaO occur even in the solid state and their kinetics are enhanced by the presence of a liquid alloys and without the need of the formation of Mg₂Ca or other Laves phases. The published thermodynamic calculations are optimized and in agreement with the solidification results from this *in situ* synchrotron radiation diffraction studies and microstructure studies. During solidification of the Mg-rich side in the Mg-Ca-O system, an invariant four-phase reaction ($\text{L} + \text{MgO} + \text{Mg} + \text{CaO}$) and non-equilibrium during solidification can explain the remaining CaO in the material. In the present case, it was not possible to analyse the volume fractions using Rietveld refinement due to the crucible material used. In order to obtain more information from the diffraction results; this should be taken into account in future studies. This data set could be better utilized for the validation of thermodynamic simulations or tomography studies.

Data availability statement

The data cannot be made publicly available upon publication because no suitable repository exists for hosting data in this field of study. The data that support the findings of this study are available upon reasonable request from the authors.

Acknowledgments

The authors acknowledge the Deutsches Elektronen-Synchrotron (DESY) in Hamburg, Germany, for the provision of synchrotron radiation facilities within the framework of the proposal I-20130330 and the Federal Ministry for Economic Affairs and Energy (BMW) for funding the project MagHyM (20K1107B).

ORCID iDs

B Wiese  <https://orcid.org/0000-0003-3094-3803>

C L Mendis  <https://orcid.org/0000-0001-7124-0544>

N Hort  <https://orcid.org/0000-0002-6636-1568>

References

- [1] Ha S H, Lee J K, Jo H H, Jung S B and Kim Shae K 2006 Behavior of CaO and calcium in pure magnesium *Rare Met.* **25** 150–4
- [2] Chase M W Jr, Davies C A, Downey J R Jr, Frurip D J, McDonald R A and Syverud A N 1985 JANAF thermochemical tables *J. Phys. Chem. Ref. Data* **14** 1–1856
- [3] Gourishankar K V, Ranjbar M K and Pierre G R S 1993 Revision of the enthalpies and Gibbs energies of formation of calcium oxide and magnesium oxide *J. Phase Equilib.* **14** 601–11
- [4] Pilling N B and Bedworth R E 1923 The oxidation of metals at high temperatures *J. Inst. Met.* **29** 529–91
- [5] Kim S K 2011 Design and Development of High-Performance Eco-Mg Alloys *Magnesium Alloys* ed F Czerwinski (IntechOpen) pp 431–68
- [6] Kim S K and Seo J H 2014 Magnesium-based alloy for high temperature and manufacturing method thereof *U.S. Patent* pp 1–19
- [7] Rafiei S, Habibolahzadeh A and Wiese B 2023 Non-ignitable dilute Mg–0.36Al–1CaO (wt.%) alloy with high compressive strength *Adv. Mater. Process. Technol.* **9** 32–46
- [8] Rafiei S, Habibolahzadeh A and Wiese B 2024 Environment-CONscious magnesium (ECO-Mg): a review *Clean. Mater.* **11** 100230
- [9] Kondoh K, Fujita J, Umeda J, Imai H, Enami K, Ohara M and Igarashi T 2011 Thermo-dynamic analysis on solid-state reduction of CaO particles dispersed in Mg–Al alloy *Mater. Chem. Phys.* **129** 631–40
- [10] Schmid-Fetzer R, Kozlov A, Wiese B, Mendis C L, Tolnai D, Kainer K U and Hort N 2016 *Thermodynamic Description of Reactions between Mg and CaO* (Magnesium Technology) pp 67–72
- [11] Liang S M, Kozlov A and Schmid-Fetzer R 2018 The Mg–Ca–O system: thermodynamic analysis of oxide data and melting/solidification of mg alloys with added CaO *Int. J. Mater. Res.* **109** 185–200
- [12] Jung I-H, Lee J K and Kim S K 2017 Mg–Ca alloys produced by reduction of CaO: understanding of ECO-Mg alloy production *Metall. Mater. Trans. B* **48** 1073–8
- [13] Tolnai D, Mendis C L, Stark A, Szakács G, Wiese B, Kainer K U and Hort N 2013 *In situ* synchrotron diffraction of the solidification of Mg₄Y₃Nd *Mater. Lett.* **102–103** 62–64
- [14] Szakacs G, Wiese B, Mendis C L, Tolnai D, Stark A, Schell N, Naira M, Kainer K U and Hort N 2014 *In Situ Synchrotron Radiation Diffraction during Solidification of Mg₄Y and Mg₄YxGd Alloys (x = 1, 4 Wt.%)* (Magnesium Technology) pp 213–8
- [15] Buzolin R H, Tolnai D, Mendis C L, Stark A, Schell N, Pinto H, Kainer K U and Hort N 2015 Investigation of compression behavior of Mg-4Zn-2(Nd, Gd)-0.5Zr at 350 °C by *in situ* synchrotron radiation diffraction *Magnesium Technology* ed M V Manuel, A Singh, M Alderman and N R Neelameggham (Springer) pp 103–7
- [16] Buzolin R H, Tolnai D, Mendis C L, Stark A, Schell N, Pinto H, Kainer K U and Hort N 2015 *In situ* synchrotron radiation diffraction study of the role of Gd, Nd on the elevated temperature compression behavior of ZK40 *Magnesium Technology* ed M V Manuel, A Singh, M Alderman and N R Neelameggham (Springer) pp 129–36
- [17] Wiese B, Mendis C L, Tolnai D, Stark A, Schell N, Reichel H P, Brückner R, Kainer K U and Hort N 2015 CaO dissolution during melting and solidification of a Mg-10 wt.% CaO alloy detected with *in situ* synchrotron radiation diffraction *J. Alloys Compd.* **618** 64–66
- [18] Wiese B, Mendis C L, Tolnai D, Szakacs G, Stark A, Schell N, Reichel H P, Bruckner R, Kainer K U and Hort N 2014 *In situ* synchrotron radiation diffraction during melting and solidification of Mg–Al alloys containing CaO *Magnesium Technology* ed M Alderman, M V Manuel, N Hort and N R Neelameggham (Springer) pp 191–5
- [19] Schell N, King A, Beckmann F, Fischer T, Müller M and Schreyer A 2014 The high energy materials science beamline (HEMS) at PETRA III *Mater. Sci. Forum* **772** 57–61
- [20] Wiese B 2016 The effect of CaO on magnesium and magnesium calcium alloys
- [21] Villars P C 2013 *Pearson's Crystal Data—Crystal Structure Database for Inorganic Compounds (On CD-ROM)* (ASM International)
- [22] Chase M W 1998 *NIST-JANAF Thermochemical Tables* 4th edn vol 9 (American Institute of Physics) pp 1–1951 (available at: www.nist.gov/publications/nist-janaf-thermochemical-tables-4th-edition)
- [23] Halstead P E and E M A 1957 769. The thermal dissociation of calcium hydroxide *J. Chem. Soc.* 3873–5
- [24] Ellingham H J T 1944 Transactions and Communications—Reducibility of oxides and sulphides in metallurgical processes *J. Soc. Chem. Ind.* **63** 125–60
- [25] Nowotny H, Mohrnhelm E G W A and Mohrnhelm A 1940 Untersuchungen in den Systemen Aluminium-Kalzium, Magnesium-Kalzium und Magnesium-Zirkon *Int. J. Mater. Res.* **32** 39–42
- [26] Rad H R B, Idris M H, Kadir M R A and Farahany S 2012 Microstructure analysis and corrosion behavior of biodegradable Mg–Ca implant alloys *Mater. Des.* **33** 88–97
- [27] Cha P R et al 2013 Biodegradability engineering of biodegradable Mg alloys: tailoring the electrochemical properties and microstructure of constituent phases *Sci. Rep.* **3** 2367
- [28] Agarwal R, Lee J J, Lukas H L and Sommer F 1995 Calorimetric measurements and thermodynamic optimization of the Ca–Mg system *Int. J. Mater. Res.* **86** 103–8
- [29] Nayeb-Hashemi A A C J B and Clark J B 1987 The CaMg (calcium-magnesium) system *Bull. Alloy Phase Diagr.* **8** 58–65
- [30] Haughton J L 1937 Alloys of magnesium. Part 6: the construction of the magnesium-rich alloys of magnesium and calcium *J. Inst. Met.* **61** 241–6
- [31] Vosskühler H 1937 The phase diagram of magnesium-rich Mg–Ca alloys *Z. Met. kd.* **29** 236–7